THE EFFECTS OF KINETICS MODELING ON MASS FRACTION PDF IN REACTING COMPRESSIBLE MIXING LAYERS

Foluso Ladeinde, Edward E. O'Brien, Wei Liu, & Michelle Nearon
Department of Mechanical Engineering
SUNY at Stony Brook
Stony Brook, L.I., New York

ABSTRACT

The effects of Mach number and the chemical kinetics scheme on the mass fraction PDF of H_2, O_2, and H_2O are investigated for turbulent, high-speed mixing layers using direct numerical simulation. The results show significant effects of these parameters.

INTRODUCTION

The use of assumed probability density functions (PDF) is common in calculations intended for generating engineering design data. It is the hope in these kinds of projects that the assumed profiles will hold for a variety of situations (Mach numbers, kinetic models, etc.). This process proves to be useful for computer-based analysis. Full kinetics modeling of the reactions are rarely feasible, not only for the fact that their details (such as the model constants) are not known, but also for the unaffordable computational costs. Therefore, engineering calculations, which deal mostly with very complex systems, commonly use substantially reduced chemistry models, in addition to the assumed PDF. The foregoing situation provides the motivation for the present studies whose precise objective is to investigate the effects of kinetic modeling on the PDF distribution and other aspects of turbulent, reacting, compressible mixing layers.

Classical references on the application of the PDF methods in reacting turbulence include O'Brien (1980) and Pope (1985), which mostly concern low Mach number flows. Studies on high speed and non-premixed chemical reactions include Drummond (1988) and the review article by Dimotakis (1991). However, these studies included neither direct numerical simulation nor the effects of different chemistry models. Givi et al. (1991) used DNS to investigate compressibility and heat release effects in a high-speed mixing layer but considered only a single step reaction. Chakraborty et al. (1997) calculated reacting mixing layers but considered only an 7-step, 8-species chemistry model.

Evans and Schexnayder (1980) studied the influence of the same chemical kinetics as in this paper (except the two-step model which they did not analyze) and of unmixedness on burning in a supersonic hydrogen flame. However, the Reynolds-averaged approach was used, with some turbulence and chemistry closure models. This differs from the rather fundamental approach in the present work, where DNS obviates the need for closure models.

DNS DETAILS

Details of the DNS model are presented in this section. Linear stability analysis for the non-reacting system shows that, for convective Mach numbers, M_c, greater than 0.6, the flow is three-dimensional at the onset of instability. However, in this paper, we will beg this issue with confinement and heat release arguments, which tend to make reacting mixing layer flows two-dimensional (2D). The resolution requirements for DNS and the shear number of partial differential equations for a multi-species reaction model also force a 2D model (Hill, 1992).

The DNS procedure in the present work is based on the ENO scheme (Ladeinde et al., 1995), with computations performed on the parallel SP/2 system under the NSF-supported NPACI program at the San Diego Supercomputing Center (SDSC). We calculate instantaneous values of density, ρ, mass flux, ρu_i, pressure, p, total energy, E, and the species mass concentrations, $\rho\phi_i$. Although fuels such as N-heptane, methane, etc., could easily be incorporated into our analysis program, we have chosen hydrogen. The oxidant is oxygen, and the overall reaction is

$$2H_2 + O_2 \underset{k_b}{\overset{k_f}{\rightleftharpoons}} 2H_2O + \text{Heat}.$$

The two-step, four-species kinetics model is:

$$H_2 + O_2 \underset{k_b}{\overset{k_f}{\rightleftharpoons}} OH$$

$$H_2 + 2OH \underset{k_b}{\overset{k_f}{\rightleftharpoons}} 2H_2O.$$

The eight-step, seven species model takes the form:

No.	Reaction
1	$H_2 + M \Leftrightarrow H + H + M$
2	$O_2 + M \Leftrightarrow O + O + M$
3	$H_2O + M \Leftrightarrow OH + H + M$
4	$OH + M \Leftrightarrow O + H + M$
5	$H_2O + O \Leftrightarrow OH + OH$
6	$H_2O + H \Leftrightarrow OH + H_2$
7	$O_2 + H \Leftrightarrow OH + O$
8	$H_2 + O \Leftrightarrow OH + H$

The twenty-five step, twelve-species kinetics model is:

No.	Reactions
1	$HNO_2 + M \Leftrightarrow NO + OH + M$
2	$NO_2 + M \Leftrightarrow NO + O + M$
3	$H_2 + M \Leftrightarrow H + H + M$
4	$O_2 + M \Leftrightarrow O + O + M$
5	$H_20 + M \Leftrightarrow OH + H + M$
6	$OH + M \Leftrightarrow O + H + M$
7	$HO_2 + M \Leftrightarrow H + O_2 + M$
8	$H_2O + O \Leftrightarrow OH + OH$
9	$H_2O + H \Leftrightarrow OH + H_2$
10	$O_2 + H \Leftrightarrow OH + O$
11	$H_2 + O \Leftrightarrow OH + H$
12	$H_2 + O_2 \Leftrightarrow OH + OH$
13	$H_2 + O_2 \Leftrightarrow H + HO_2$
14	$OH + OH \Leftrightarrow H + HO_2$
15	$H_2O + O \Leftrightarrow H + HO_2$
16	$OH + O_2 \Leftrightarrow O + HO_2$
17	$H_2O + O_2 \Leftrightarrow OH + HO_2$
18	$H_2O + OH \Leftrightarrow H_2 + HO_2$
19	$O + N_2 \Leftrightarrow N + NO$
20	$H + NO \Leftrightarrow N + OH$
21	$O + NO \Leftrightarrow N + O_2$
22	$NO + OH \Leftrightarrow H + NO_2$
23	$NO + O_2 \Leftrightarrow O + NO_2$
24	$NO_2 + H_2 \Leftrightarrow H + HNO_2$
25	$NO_2 + OH \Leftrightarrow NO + HO_2$

The twelve species in the most complex model are: H, O, H_2O, OH, O_2, H_2, N_2, N, NO, NO_2, HO_2, and HNO_2. The Arrhenius approach is used to model the reaction rates for the steps; the constants in the various models can be found in Evans and Schexnayder (1980), except for the 2-step reaction whose constants are available in Vullermoz et al. (1992).

PARAMETER RANGE AND THE INITIAL AND BOUNDARY CONDITIONS

The mixing layer model in this work is of the temporal type and the mean velocity is initialized with the hyperbolic tangent profile. Taking the M_c = 0.8 case as an example (sound speed c = 340 m/s), the parameter set in the equations is: Re = 400, Pr = 1.4, Ce = 1.5, Sc = 0.5. The reference variables are: U = 272 m/s, L = 0.001 m, T_{Ref} = 2000 K, ρ_{Ref} = 0.1765 kg/m^3 (density of air at T_{Ref}). The specific initial mean velocity profile in all cases is $\bar{u} = \tanh(2y)$, where y is the traverse coordinate. The streamwise coordinate is denoted by x. The initial mean temperature profile is calculated using the Crocco-Buseman relation. A mean pressure of unity is assumed for the mean flow and the initial density is obtained via the equation of state. The perturbation velocities are as presented in Ladeinde et al. (1999).

The initial conditions for the species are given by

$$\phi_{H_2} = 0.4(1+\tanh(2y)), \phi_{O_2} = 0.8 - \phi_{H_2},$$

$$\phi_{N_2} = 0.2, \phi_{Others} = 0$$

so that the mass concentrations of all species will add up to 1 initially. This is the case for the 8- and 25-step reactions, which both involve nitrogen as an inert gas. The initial conditions for the 2-step reaction are discussed later in this paper. For boundary conditions, periodicity is assumed streamwise and zero gradient free-stream. This is the case for all primary dependent variables in the governing equations. Finally, no numerical "spark-plug" was implemented in these studies; the approaching streams seem to possess a high enough temperature (2000K) for "spontaneous" reaction.

Finally, the convective Mach numbers, M_c, presented in this paper are 0.2, 0.5, and 0.8. Note that each of the steps in the reactions possesses its own effective Damkholer number and the various species, in general, have different diffusivities (Schmidt numbers). These parameters were not varied in the simulations.

The computational domain is (x,y) $\in$ (0, 20) X (-50, 50). The grid size for the numerical calculations is determined from the Kolmogorov scales, not the Batchelor scales. Most of the calculations are done on a 256^2 grid, with a few on 128^2 and 512^2.

RESULTS AND DISCUSSION

The results shown in Figures 1 through 5 illustrate the effects of the kinetics model on the PDF and the dynamics of the system in question. In Figures 1 (a) and (b), the layer growth rate for reacting and non-reacting flows, are shown as functions of the eddy turn over time, $t_e = t\Delta U/\delta_o$, where t is the non-dimensional simulation time, ΔU is velocity difference between the top and bottom streams, and δ_o is the initial vorticiy thickness. It is evident that both the Mach number and the kinetics model affect the layer thickness. From Fig. 1 (b), it can be observed that chemical reaction affects the growth rate by as much as 6% (8-step) and 13% (25-step). The figure also shows superposed oscillations over the profile for the non-reacting case. The oscillations appear correlated for the two reacting cases, as shown by the points A-B-C-D-E in the 8-step reaction system and the corresponding points A'-B'-C'-D'-E' in the 25-step reacting system. The 2-step reaction model generates a growth rate that is similar to that for the non-reacting flow, when M_c = 0.8.

The contour maps of water concentration are shown in Figure 3 for the three kinetics models and M_c = 0.5. The distributions are similar for the various kinetics models, although the details of the interior are different. The 25-step reaction shows the largest gradient in the interior of the cell, followed by the 8-step reaction and then the 2-step reaction. The center

concentration values are significantly different at 0.336, 0.166, and 0.253 respectively. This shows that the 25-step kinetics model leads to a vigorous reaction and production of H_2O for this $M_c = 0.5$ case. Figure 3 (b) also supports this statement. As Fig. 3 (a) shows, the extent of reaction is particularly low for the 8-step reaction when $M_c = 0.2$. However, when $M_c = 0.8$, reaction in the 8-step scheme seems to be stronger than that in the 2-step scheme, but still weaker than that for the 25-step scheme.

Figure 4 shows the normalized temperature profile:

$$\theta(y) = \frac{T(y) - T_\infty}{(T_{ad} - T_\infty)},$$

where T_∞ is the temperature of the unreacted mixtures and T_{ad} is the adiabatic flame temperature, for which we have used the maximum temperature, which occurs around $y = 0$. The time evolution of this profile has been reported in Ladeinde et al. (1999) for the 8- and 25-step models. A strange development in the $M_c = 0.5$ and 0.8 cases can be observed, whereby energy is being drawn from the system, as manifested in temperature values which are lower than that in the unreacted streams. Our first reaction was to attribute the observation to numerical difficulties. However, a rigorous diagnosis, including grid refinement, didn't support a numerical artifact. So, we conclude that the phenomenon, which didn't show up in the $M_c = 0.2$ systems, was probably a true reflection of the physics. Some endothermic reaction steps are the likely cause of this phenomenon.

Each direction in ϕ space is divided into 100 intervals for the purpose of calculating the PDF, $P(\phi_i)$. Because these intervals $(\Delta\phi_i)$ are uniform for each species, the plots can be interpreted in terms of the probability, $P(\phi_i)\ \Delta\phi_i$. The initial conditions for H_2 and O_2 are the same for all calculations of the 8- and 25-step kinetics models. However, the 2-step model does not involve nitrogen (inert) and so matching the initial concentrations of the 8-step and 25-step cases, which ideally is what should be done to enable comparison, will require that the mass fractions do not add up to unity. The effects of this mismatch in the initial concentration were studied. In one case, for the 2-step scheme, the conditions were $\phi = 0.4$ for H_2 and O_2; in another, it was $\phi = 0.5$. Figures 5 (d) through (f) used the former conditions, whereas Figures (g) through (I) used the latter. It should be noted that the PDF plots are for y=0.

The PDF profile for the 8-step reaction will be discussed first. Figures 5 (a) through (c) represent the lowest Mach number case ($M_c = 0.2$). The relatively tall peaks show that the 8-step kinetics model is characterized by a fairly high level of mixing. However, from the centered location of the peaks along the ϕ coordinate direction, we see that there is virtually no reaction for this model and Mach number. The dark portion of Figure 5 (c) is a result of the concentration of lines in that low water concentration region, supporting the observation that the 8-step kinetics model does not lead to much reaction. The PDF profiles for $M_c = 0.5$ are different from those for $M_c = 0.2$, again for the 8-step reaction. Figure 5 (d) shows more reaction although the extent of mixing is lower. The higher product formation in Figure 5 (f) supports these statements, although low values of water are more probable. The $M_c = 0.8$ case shows even more reaction than for $M_c = 0.5$.

For the 25-step scheme, there is, in general, very little mixing when $M_c = 0.2$, although there seems to be a strong reaction at this Mach number. The mixing level is even lower at $M_c = 0.5$ but the extent of reaction is significant. For $M_c = 0.8$, there is an unexpectedly high mixing of O_2, although the mixing of H_2 is quite modest. For $M_c = 0.5$, the 2-step scheme shows a similar mixing strength as the 25-step scheme and the reaction is such that high concentrations of H_2O are more probable. For the 2-step scheme, the $M_c = 0.8$ case shows better mixing than for $M_c = 0.5$. These PDF results are supported by the results in Figures 1 through 5.

ACKNOWLEDGEMENT

The authors acknowledge NSF funding (CTS-9626413) for this study.

REFERENCE

Chakraborty, D., Nagaraj Upadhyaya, H. V., Paul, P. J., and Mukunda, H. S., 1999, Phys. Fluids, Vol. 9, pp. 3513-3522.

Dimotakis, P. E., 1991, In *High-Speed Flight Propulsion Systems*, Edit. S.N.B. Murthy & E.T. Curran, Vol. 137 of Progress in Aeronautics and Astronautics. Publ. AIAA.

Drummond, J.P., 1988, NASA Technical Memorandum 4055, December 1988.

Givi, P., Madnia, C.K., Steinberger, C.J., Carpenter, M.H., and Drummon, J.P., 1991, Combust. Sci. and Tech., Vol. 78, 1991, pp. 33-67.

Evans, J.S. and Schexnayder, C.J.,1980, AIAA Journal, Vol. 18, No 2, pp. 188-193.

Higuera, F.J. & Moser, R.D., *Proc. 1994 Summer Program*, CTR.

Hill, J. C. 1992. Proc. 1992 Summer Program, CTR, pp. 425.

Ladeinde, F. Liu, W., & O'Brien, E. E., 1999, AIAA-99-0413.

Ladeinde, F., O'Brien, E. E., Cai, X. & Liu, W. *Phys. Fluids*, Vol. 7, No. 11, 1995, pp. 2848-2857

Vullermoz, P., Oran, E. S., and Kailasanath, K. 1992, 24th Symposium on Combustion, pp. 355-403. The Combustion Institute.

Williams, F.A., 1985, Combustion Theory Bengam/Cummings Publishing Co., Menlo Park, California, 1985.

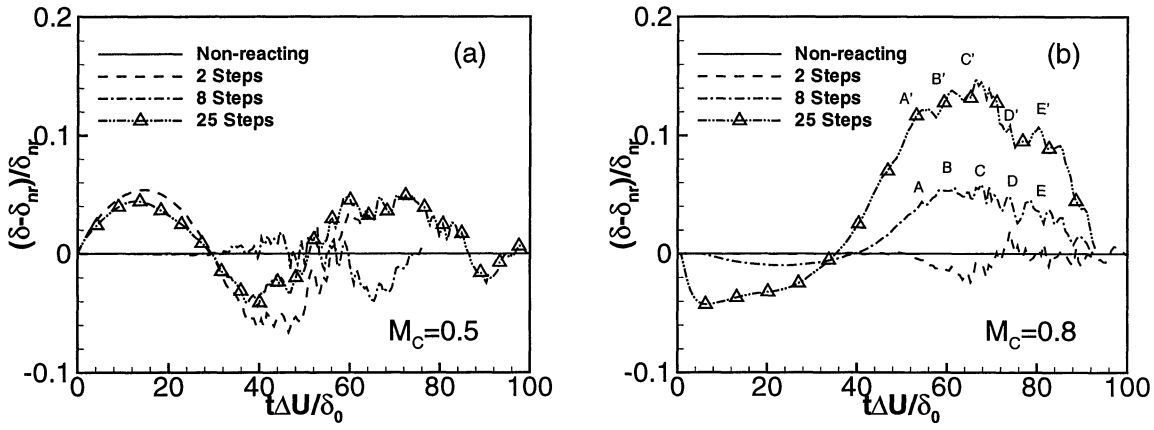

Figure 1: Vorticity thickness relative to value for non-reacting flow

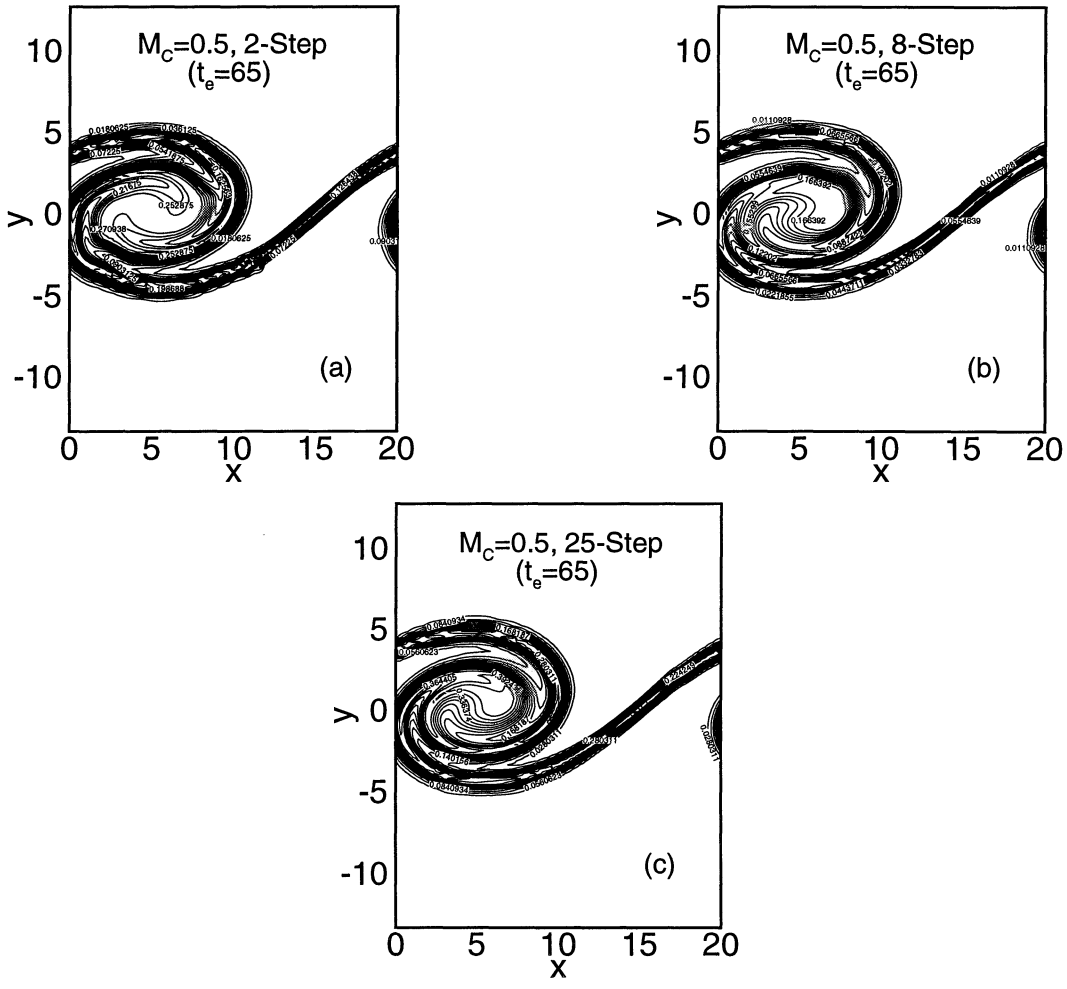

Figure 2: Contour maps of water mass fraction as a function of the kinetic model.

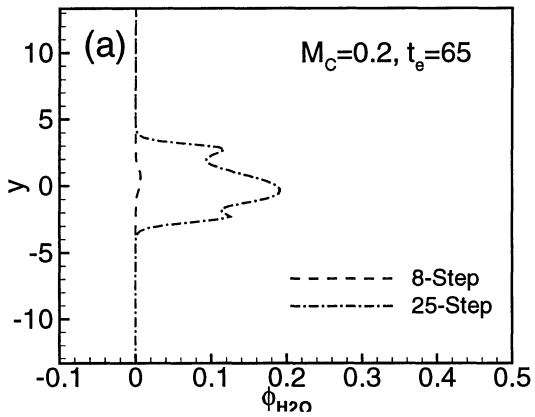

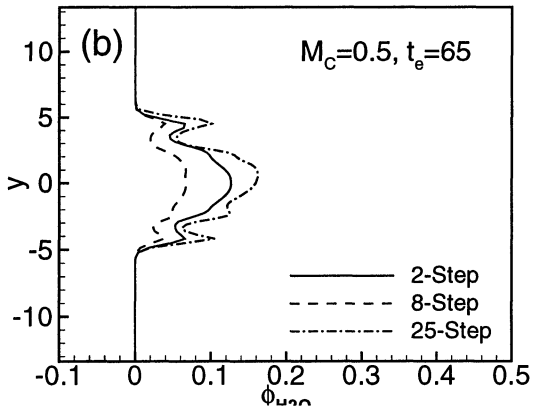

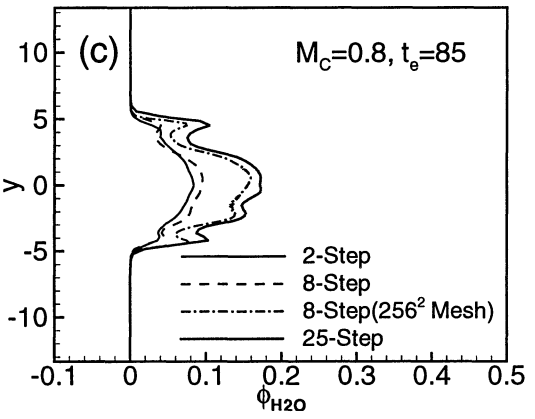

Figure 3: Horizontally-averaged water mass fraction

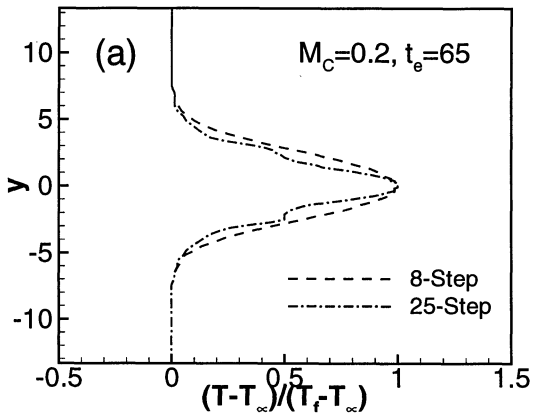

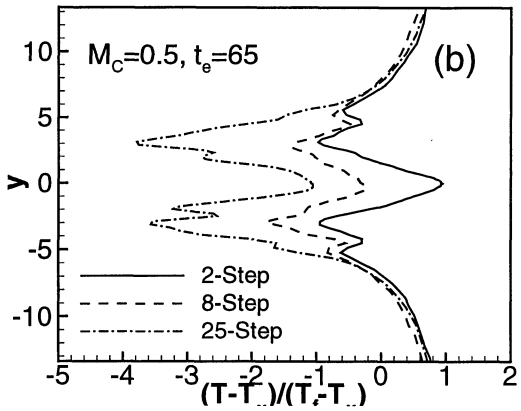

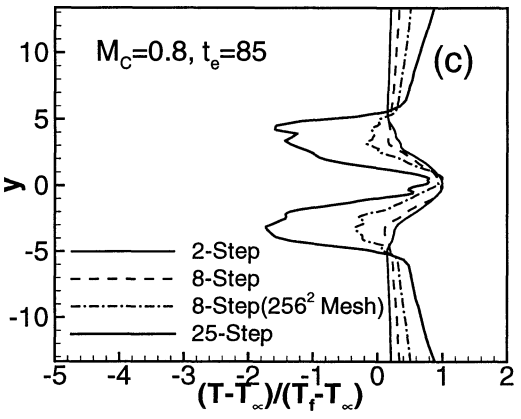

Figure 4: Horizontally-averaged temperature profile

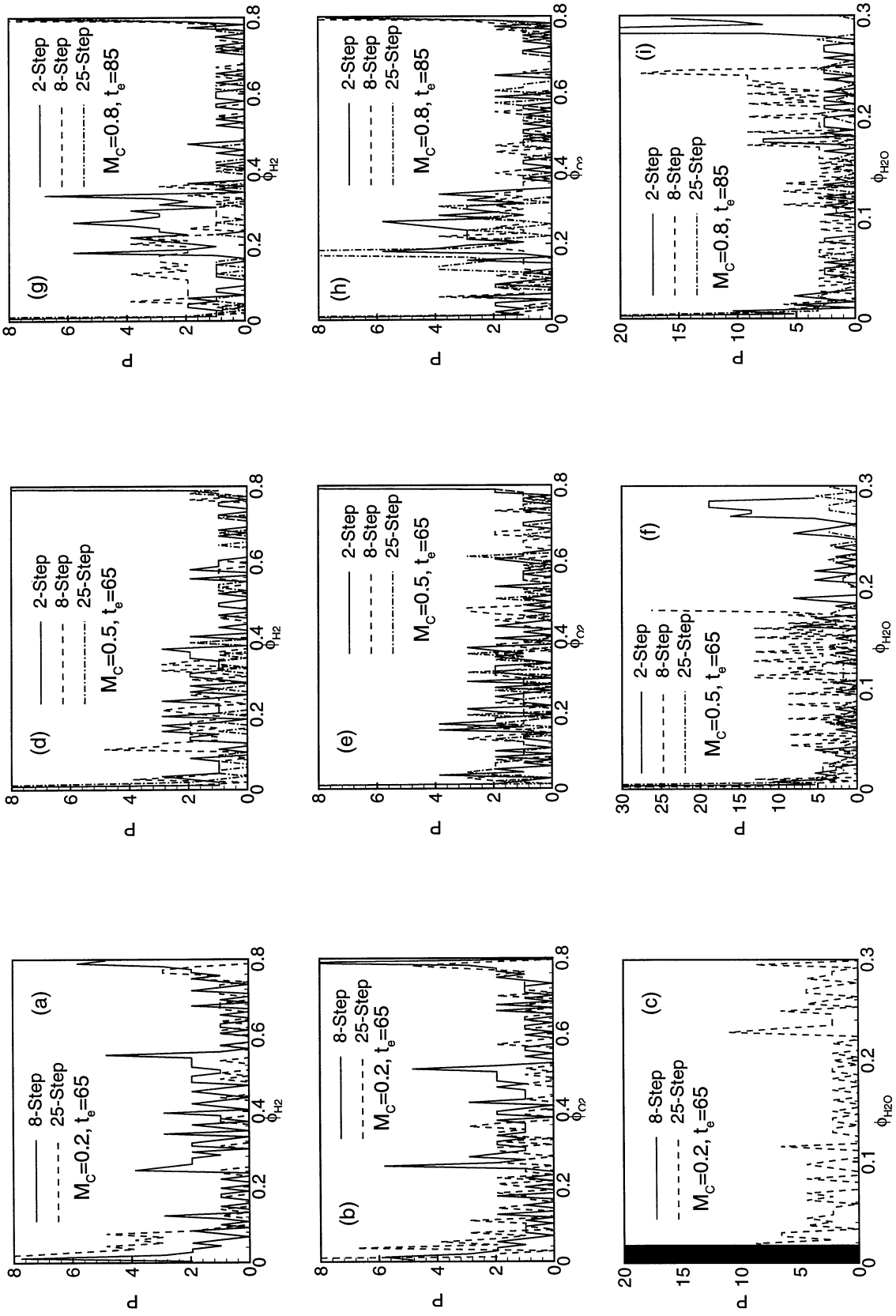

Figure 5: PDF profiles.